

# Peroxisome Proliferator-activated Receptor- $\gamma$ Down-regulates Chondrocyte Matrix Metalloproteinase-1 via a Novel Composite Element\*

Received for publication, November 20, 2003, and in revised form, April 15, 2004  
Published, JBC Papers in Press, April 16, 2004, DOI 10.1074/jbc.M312708200

Mathias François‡, Pascal Richette‡, Lydia Tsagris‡, Michel Raymondjean‡,  
Marie-Claude Fulchignoni-Lataud‡, Claude Forest‡, Jean-François Savouret‡,  
and Marie-Thérèse Corvol‡¶

From ‡INSERM UMR-S-530, Université Paris 5, UFR Biomédicale, 45 Rue des Saints Pères, 75006 Paris and  
§CNRS UMR 7079, 7 Quai Saint Bernard, 75005 Paris, France

Interleukin-1 $\beta$  (IL-1 $\beta$ ) induces degradation via hyperexpression of an array of genes, including metalloproteinases (MMP), in cartilage cells during articular degenerative diseases. In contrast, natural ligands for peroxisome proliferator-activated receptors (PPARs) display protective anti-cytokine effects in these cells. We used the PPAR agonist rosiglitazone (Rtz) to investigate PPAR- $\gamma$  isotype on IL-1 $\beta$ -target genes. Immunocytochemistry, electrophoretic mobility shift, and transient transfection assays revealed a functional PPAR- $\gamma$  in chondrocytes *in vitro*. Rtz displayed significant inhibition of IL-1 $\beta$  effects in chondrocytes. Low Rtz concentrations (close to  $K_d$  values for PPAR- $\gamma$ , 0.1 to 1  $\mu$ M) inhibited the effects of IL-1 $\beta$  on <sup>35</sup>S-sulfated proteoglycan production and gelatinolytic activities and down-regulated MMP1 expression at mRNA and protein levels. We have investigated the mechanism of action of Rtz against IL-1 $\beta$ -mediated MMP1 gene hyperexpression. Rtz effect occurs at the transcriptional level of the MMP1 promoter, as observed in transiently transfected cells with pMMP1-luciferase vector. Transient expression of wild type PPAR- $\gamma$  enhanced Rtz inhibitory effect in chondrocytes, whereas a mutated dominant negative PPAR- $\gamma$  abolished it, supporting the role of PPAR- $\gamma$  in this effect. MMP1 gene promoter analysis revealed the involvement of a *cis*-acting element located at -83 to -77, shown to be a composite PPRE/API site. Gel mobility and supershift assays demonstrated that PPAR- $\gamma$  and c-Fos/c-Jun proteins bind this *cis*-acting element in a mutually exclusive way. Our data highlight a new PPAR- $\gamma$ -dependent inhibitory mechanism on IL-1 $\beta$ -mediated cartilage degradation occurring through DNA binding competition on the composite PPRE/API site in the MMP1 promoter.

Peroxisome proliferator-activated receptor  $\gamma$  (PPAR- $\gamma$ )<sup>1</sup> natural ligands, such as 15-deoxy- $\Delta$ 12,14-prostaglandin J2 (15d-

\* This work was supported by INSERM and by the Association de Recherche sur la Polyarthrite (Paris, France). The costs of publication of this article were defrayed in part by the payment of page charges. This article must therefore be hereby marked "advertisement" in accordance with 18 U.S.C. Section 1734 solely to indicate this fact.

¶ To whom correspondence should be addressed. Tel.: 33-1-42-86-38-71; Fax: 33-1-42-86-38-68; E-mail: maite.corvol@univ-paris5.fr.

<sup>1</sup> The abbreviations used are: PPAR- $\gamma$ ,  $\gamma$  isotype of peroxisome proliferator-activated receptor; DMEM, Dulbecco's modified Eagle medium; EMSA, electrophoretic mobility shift assay; FCS, fetal calf serum; IL-1, interleukin 1; MMPs, matrix metalloproteinases; PG, proteoglycans; rosiglitazone, Rtz; PPRE, peroxisome proliferator-activated responsive element; PMA, phorbol 12-myristic-13-acetate; 15d-PGJ2, 15-

PGJ2), exert anti-IL-1 $\beta$  effects in cartilage cells *in vivo* and *in vitro*. Intra-articular injection of 15d-PGJ2 inhibits adjuvant-induced arthritis in rats (1) and addition of 15d-PGJ2 to IL-1 $\beta$ -treated human or rat chondrocytes in culture counteracts IL-1 $\beta$ -induced effects (2–4). As IL-1 $\beta$  plays a central role in the degradation of cartilage in rheumatoid arthritis and osteoarthritis (5, 6), the above data suggest a role for PPAR- $\gamma$  in cartilage homeostasis leading to new directions in therapeutic research.

PPAR- $\gamma$  is a member of the nuclear receptor superfamily of ligand-dependent transcription factors. PPAR- $\gamma$  forms a heterodimeric complex with the retinoid X receptor (7) and binds to specific nucleotide motifs (direct repeats with single spacing, DR1) located in the promoter of target genes. Natural ligands such as 15d-PGJ2 have been shown to activate PPAR- $\gamma$ , yet the true physiological ligands of this receptor remain elusive. Numerous synthetic PPAR- $\gamma$  activators have been identified, including thiazolidinediones (such as rosiglitazone (Rtz)) used in the treatment of type II diabetes (8). PPAR- $\gamma$  was first demonstrated to regulate adipocyte differentiation, and it has been recognized recently (9) to be implicated in the modulation of cancer cells growth and inhibition of the inflammatory process in immunocompetent cells (10–13) and other cell types (14), including cartilage cells (2–4). Most anti-inflammatory effects have been observed with 15d-PGJ2, a poor agonist of PPAR- $\gamma$ , whereas synthetic PPAR- $\gamma$  ligands such as Rtz were less effective or not active, despite their higher affinity for the receptor (Rtz  $K_d \leq 100$  nM). Thus, the question regarding the exact role and the implication of PPAR- $\gamma$  in these effects has been largely discussed and documented in cells from the immune system. Overexpression of PPAR- $\gamma$  in macrophages maximized the ability of diverse PPAR- $\gamma$  agonists to inhibit the expression of inflammatory response genes consistent with a PPAR- $\gamma$ -mediating anti-inflammatory mechanism (15, 16). Other data indicated PPAR- $\gamma$ -independent anti-inflammatory effects. Treatment of macrophages derived from PPAR- $\gamma$ -null embryonic stem cells with high concentrations of synthetic PPAR- $\gamma$  ligands was reported recently (17) to inhibit the induction of the inducible nitric-oxide synthase and COX2. Similar data were observed in the RAW 264.7 macrophages (18–20).

In sharp contrast, the role of Rtz-activated PPAR- $\gamma$  as an antagonist of IL-1 $\beta$ -induced cartilage degradation is largely unknown. The aim of this work was to analyze this role through the effects of the hypolipidemic drug rosiglitazone on IL-1 $\beta$ -induced target genes active in the degradative process of

deoxy- $\Delta$ 12,14-prostaglandin J2; PBS, phosphate-buffered saline; RT, reverse transcriptase; DN, dominant negative; NF $\kappa$ B-RE, nuclear factor  $\kappa$ B-responsive element.

matrix proteins synthesized by culture chondrocytes. We report a PPAR- $\gamma$ -dependent inhibitory mechanism on IL-1 $\beta$ -induced MMP1 expression acting through a new composite PPRE/AP-1 site at positions -83 to -71 upstream from the MMP1 rabbit gene transcription start site.

#### EXPERIMENTAL PROCEDURES

**Isolation and Culture of Chondrocytes from Rabbit Articular Cartilage**—Articular chondrocytes were cultured as described previously (21). Briefly, 5-week-old Fauve de Bourgogne rabbits (CPA, Orleans, France) were killed, and the femoral, humeral, and tibial articular cartilages were removed under sterile conditions. Thin slices of cartilage were sequentially digested with 0.2% hyaluronidase and 0.2% collagenase in Geys' balanced salt solution (Eurobio, Les Ulis France). The resulting cell suspension was plated at  $10^5$  cells per  $\text{cm}^2$  (high density) into 75- $\text{cm}^2$  flasks or 6-well plates and incubated in Ham's F-12 medium (Invitrogen) containing 10% fetal calf serum (FCS), 100 IU/ml penicillin, and 100  $\mu\text{g}/\text{ml}$  streptomycin. Cells were then cultured at 37 °C in an atmosphere of 8%  $\text{CO}_2$  in air, and the medium was changed once until the cells were confluent (day 6 of the primary culture). The medium was replaced with 2% FCS/Dulbecco's modified Eagle's medium (DMEM) (Invitrogen) to which was added either IL-1 $\beta$  alone (Immugenex Corp., Los Angeles) or combined with Rtz at concentrations ranging between 0.1 and 10  $\mu\text{M}$ . Cells were incubated for 18 h and analyzed as below.

**Immunological Studies**—Chondrocytes were cultured in 4-chamber labtek slides (Merck) and incubated for 18 h in 2% FCS/DMEM with or without 1  $\mu\text{M}$  Rtz. After being washed in PBS, cells were fixed with 4% paraformaldehyde in 0.1 M sodium phosphate and washed in blocking buffer (PBS with 5% bovine serum albumin and 0.2% Tween 20). Fixed cells were then exposed to polyclonal PPAR- $\gamma$  antibody (Santa Cruz Biotechnology) diluted at 1:100 in blocking buffer for 2 h at room temperature (20 °C) in a humid chamber. After a quick rinse in 0.1% PBS/Tween, cells were exposed to the rabbit anti-goat Alexa 546-coupled secondary antibody (Molecular Probes and Invitrogen) diluted at 1:800 for 2 h. Cells were rinsed in PBS/Tween and mounted with Vectashield. The slides were observed with a Nikon Labophot 2 and photographed with a Spot camera driven by the Spot Jr software (Diagnostic Instrument). Controls were made by omission of primary antibody.

**Nuclear Extract and Electrophoretic Gel Mobility Shift Assay (EMSA)**—Nuclear proteins were extracted as described by Riquet *et al.* (22). Briefly, cells were treated with various effectors for 60 min and then scraped on ice and washed twice in a PBS solution. After a centrifugation at  $800 \times g$  for 5 min at 4 °C, the pellet was dissolved in an RSB 1 $\times$  buffer (10 mM Tris, 10 mM NaCl, 3 mM  $\text{MgCl}_2$ , 0.002%  $\text{NaN}_3$ ) plus 0.5% Nonidet P-40 with a protease mixture inhibitor (Roche Applied Science). This step was repeated once. Cell lysate was centrifuged at  $5100 \times g$  for 5 min at 4 °C. The pellet was dissolved in buffer C (20 mM Hepes, pH 7.4, 420 mM NaCl, 25% glycerol, 1.5 mM  $\text{MgCl}_2$ , 0.2 mM EDTA, 0.01%  $\text{NaN}_3$ ). After a 30-min incubation, nuclear proteins were centrifuged at  $105,000 \times g$  for 15 min at 4 °C. The supernatant was mixed with an equal volume of buffer D (20 mM Hepes, 50 mM KCl, 0.2 mM EDTA, 0.01%  $\text{NaN}_3$ ), collected, and stored in liquid nitrogen. Double-stranded oligonucleotide was labeled by the Klenow fragment of DNA polymerase in the presence of [ $\alpha$ - $^{32}\text{P}$ ]dCTP. Samples of 6  $\mu\text{g}$  of each nuclear extract were incubated with 50 fmol of double-stranded radiolabeled oligonucleotides in 6  $\mu\text{l}$  of EMSA mix (50 mM Hepes, pH 7.9, 50% glycerol, 5 mM EDTA, and 300 mM KCl) plus 1  $\mu\text{g}$  of polyd(I-C), 600 ng of bovine serum albumin, 10 mM dithiothreitol, 1.5 ng of salmon sperm DNA in a final volume of 15  $\mu\text{l}$ . Incubation was performed for 20 min at room temperature. The samples were analyzed by electrophoresis in 6 or 8% denaturing polyacrylamide gels containing, respectively, 1 or 0.25 $\times$  TBE for 180 min at 130 V, transferred to 3MM paper (Whatman), dried under vacuum at 80 °C, and exposed to biotech x-ray film (Amersham Biosciences). To determine the specificity of the DNA protein complex, competition assay was performed using a 50- or 100-fold molar excess of the corresponding unlabeled, double-stranded oligonucleotide. PPAR- $\gamma$  (sc-1984X), PPAR- $\beta$  (sc-1983X), and PPAR- $\alpha$  (sc-1985X) goat polyclonal antibodies, p50 goat polyclonal antibody (sc-1190X), p65 mouse monoclonal antibody (sc-8008X), Fos (253X), Fra-1 (sc-183X), Fra-2 (sc-171X), c-Fos (sc-52X), and c-Jun (sc-45X) rabbit polyclonal antibodies were purchased from Santa Cruz Biotechnology (Tebu, France). For supershift analysis, antibodies were added (2  $\mu\text{g}$ ) to the incubation for 15 min at 4 °C before the binding reaction. Three double-stranded oligonucleotides were constructed, containing either the canonical PPRE site from the acyl-CoA oxidase gene, 5'-AGCTGGACCAGGACAAAGGTCACGTT-3', the composite PPRE/AP-1 element 5'-GGATCCTATAAAGCATGAGTCCACAGCCCTCAGCT-3' at -83 to

-71 in the rabbit MMP1 gene, or the NF- $\kappa\text{B}$  site at -3029 to -2994 5'-GGGAATTGAATATGGAAAAACACCAACATAGTTGAG-3' (23).

**Transient Transfection and Luciferase Assay**—Rabbit chondrocytes were cultured in Ham's F-12 containing 10% FCS as described above, trypsinized, and plated in 6-well plates. Cells were then transfected at 70% confluence via a calcium phosphate precipitation method. Briefly, cells were incubated for 4 h with the precipitate obtained with 0.02 M  $\text{CaCl}_2$  in a Hepes buffer, pH 7.0, and 1.5  $\mu\text{g}$  of DNA/well, *i.e.* either by adding 1  $\mu\text{g}$  of the 3xPPRE-TK-Luc construct (a gift from Dr. P. Grimaldi, Nice, France) or the chimeric MMP1 promoter-luciferase construct with 500 ng of  $\beta$ -galactosidase expression vector. Each point was made in triplicate. Cells were then lysed in 400  $\mu\text{l}$  of lysis buffer (Promega, France). Luciferase assay was performed using 20  $\mu\text{l}$  of cell lysis on a Lumat LB 9507 luminometer (Berthold, France). Efficiency of the transfection was shown to be 50–70% of total cells, as determined by  $\beta$ -galactosidase assay (Promega, France).

**Measurement of [ $^{35}\text{S}$ ]Sulfate Incorporation into Proteoglycans (PG)**—The incorporation of [ $^{35}\text{S}$ ]sulfate into PG by articular chondrocytes was assessed as described previously (24). At confluency, chondrocytes were incubated in 2% FCS/sulfate-free DMEM plus 1.5  $\mu\text{Ci}/\text{ml}$   $\text{Na}_2^{35}\text{SO}_4$  (75 MBq/ml, Amersham Biosciences) for 18 h in the presence or absence of effectors. Controls were prepared without any additive compound. Each point was prepared in triplicate. Proteoglycans were extracted from culture media and cell layer at 4 °C by incubation with 3 M guanidinium chloride in 0.05 M Tris-HCl (Merck), pH 7.4, in the presence of protease inhibitors (10 mM  $\text{Na}_2\text{EDTA}$  (Sigma), 5 mM benzamidine (Merck), and 0.1 mM 6-aminohexanoic acid (Prolabo, Fontenay, Bois, France)). Aliquots of the guanidinium extract were then spotted on a set of Whatman 3MM paper and allowed to dry. The set was used to quantify total high molecular weight/highly charged sulfated PG subunits, which were precipitated with 5% cetylpyridinium chloride in 0.3 M NaCl (Sigma) according to Larsson and Kuettner (25). Scintillation liquid was added to each strip, and the strips were counted in a Packard tricar  $\beta$ -spectrometer. Each measurement was made in triplicate. For each experiment, the amount of DNA was measured in sister flasks by the fluorometric method described by Kapuscinski and Skoczylas (26). Results were calculated as mean  $\pm$  S.D. cellular or medium dpm/10  $\mu\text{g}$  of DNA of four similarly treated wells. Results are presented as total radiolabeled PG expressed in percent of controls performed with cells from three different animals.

**Zymography**—Zymographic analysis of gelatinase activities was performed by using cell culture supernatants (10  $\mu\text{l}$ ). The chondrocyte-conditioned medium, mixed with 4 $\times$  sample buffer (250 mM Tris base, 2.5% SDS, 12.5% glycerol, 0.1% bromophenol blue), was subjected to electrophoresis at 4 °C on a 0.1% SDS-polyacrylamide gel containing 1 mg/ml gelatin. After electrophoresis, the SDS was removed by washing the gel in a 2.5% Triton X-100 for 30 min with one change of the incubating buffer. The gel was then incubated at 37 °C for 24 h in incubation buffer (50 mM Tris-HCl, pH 7.4, 5 mM  $\text{CaCl}_2$ , 0.02%  $\text{NaN}_3$ , 1  $\mu\text{M}$  ZnCl $_2$ , 0.0015% Brij-35, 2.5% Triton X-100). Gels were stained with 0.5% Coomassie Blue, 10% acetic acid, 30% methanol buffer and destained with sequential discoloration solutions until the digested bands were clearly separated. A molecular marker was electrophoresed. The levels of the 92-, 72-, and 53/58-kDa gelatinolytic activities were quantified by video densitometry.

**Western Blotting**—Proteins were extracted from culture medium by addition of 5 volumes of cold acetone and centrifuged at  $12,000 \times g$  for 5 min. The pellet was collected in 10 mM phosphate buffer containing protease inhibitors. Proteins were size-separated by SDS-PAGE in 10% polyacrylamide gel. A Colored Rainbow mix, code RPN 756 (Amersham Biosciences), was used as the molecular weight marker. The gel was electroblotted to nitrocellulose (Bio-Rad) in transfer buffer (25 mM Tris-HCl, 192 mM glycine, pH 8.3) in a Transblot Cell (Bio-Rad). Equal transfer of proteins was confirmed by staining the nitrocellulose with Ponceau Red (0.2% w/v  $\text{H}_2\text{O}$  diluted 99:1 in 10% trifluoroacetic acid). The MMP1 antibody (polyclonal goat anti-human MMP1, Santa Cruz Biotechnology (Tebu, France)) was diluted at 1:200 and used as primary antibody overnight at 4 °C. A peroxidase-conjugated rabbit anti-goat IgG (Dako P0160) was used as secondary antibody at 1:2000 and incubated for 1 h at room temperature. Blots were revealed by enhanced chemiluminescence as instructed by the manufacturer (ECL, Amersham Biosciences). Semi-quantitative scanning densitometry was performed with the NIH image software (results were standardized using Ponceau Red staining for homogeneity).

**Production of Rabbit cDNA Probes by RT-PCR**—MMP probes were generated by RT-PCR in accordance with the human sequences, selected in a domain conserved across species for MMP1, MMP3, and MMP13 (GenBank<sup>TM</sup> accession numbers M17821, M25664, and

M002427, respectively). Total RNA was prepared from control or IL-1 $\beta$  (10 ng/ml)-treated rabbit chondrocytes and synthesized into cDNA using Moloney murine leukemia virus-reverse transcriptase (Promega). Briefly 1  $\mu$ g of total RNA was reverse-transcribed at 42 °C for 1 h in a 25- $\mu$ l reaction according to the manufacturer's instructions. The resulting cDNA was amplified for PCR on a DNA thermal cycler (PerkinElmer Life Sciences) using the following program: 96 °C for 5 min, followed by 35 cycles of 96 °C for 30 s, 55–60 °C for 30 s, and 72 °C for 1 min. A 15-min 72 °C extension step completed the reaction. PCR products were subcloned in pGEM vector.

**Rabbit MMP1 Promoter Cloning**—Genomic DNA from rabbit chondrocytes was extracted by Trizol (Invitrogen), according to the supplier's instructions. MMP1 promoter primers were chosen in the GenBank™ accession number M17820: 5'-CGGGGTACCGACCAAGGACTCAAGA-3' and 5'-ACTGAGAAGGAAGACACTCGAGCGG-3'. A proofreading Taq (*Pfu* Turbo, Stratagene, France) was used for PCR with the long range method (hot start: 96 °C, 5 min), 10 cycles ((98 °C, 30 s; 57 °C, 1 min; 72 °C, 5 min)), 20 cycles ((98 °C, 30 s; 57 °C, 1 min; 72 °C, 5 min with an incrementation of 20 s per cycle)), and terminal extension at 72 °C for 10 min. The 3.5-kb MMP1 promoter fragment was purified with GeneClean Sprint kit (Bio 101) and inserted in pGL3-basic vector (Promega, France) using KpnI and XhoI restriction sites.

**Mutagenesis**—All mutants were generated with the Quick Change site-directed mutagenesis kit from Stratagene (France). The dominant negative PPAR- $\gamma$  was constructed following the procedure (27) described by Gurnell *et al.* (28) in which Leu<sup>468</sup> and Glu<sup>471</sup> were mutated to alanine in the ligand binding domain. A double point mutation (AAAGCA to AGTAGT) was introduced into the proximal PPRE-like site -83 to -78 to generate the pGL-MMP1- $\Delta$ PPRE, by using the forward sequence primer 5'-TCAAGAGGATGTTATAGTAGTTGAGT-CACACAGC-3', corresponding to region -99 to -65 of the rabbit MMP1 promoter.

**DNA Sequencing**—Automated sequencing was performed by Genome Express to confirm the identity of all DNA probes and constructs used in the study.

**RNA Isolation and Northern Blot**—Total RNA was extracted from cells by a single-step method using Trizol reagent (Invitrogen). Samples of 10  $\mu$ g of total RNA were used for Northern blot analysis. The rabbit MMP1, -3, and -13 cDNA probes were synthesized by RT-PCR. All probes were labeled by random priming with [ $\alpha$ -<sup>32</sup>P]dCTP (Amersham Biosciences) to a specific activity of 10<sup>8</sup> to 10<sup>9</sup> cpm/ $\mu$ g. Results were normalized by using a human glyceraldehyde-3-phosphate dehydrogenase probe and quantified using Studio Scan II (Agfa, Paris, France) with the NIH software.

**Statistical Analysis**—Values are expressed as the mean  $\pm$  S.D. Statistics were performed by analysis of variance. Multiple comparisons were performed with the Tukey test. Differences between groups were considered significant for  $p \leq 0.05$ .

## RESULTS

**Presence of Functional PPAR- $\gamma$  in Cultured Articular Chondrocytes**—PPAR- $\gamma$  displayed nuclear localization in our *in vitro* model of cultured rabbit chondrocytes, independently of Rtz treatment (Fig. 1A). EMSA was carried out with nuclear extracts from 1  $\mu$ M Rtz-treated chondrocytes and an oligonucleotide containing the canonical PPRE sequence described under "Experimental Procedures." Fig. 1B showed the involvement of the PPRE-containing oligonucleotide in a robust protein-DNA complex. Binding specificity was confirmed by using an 80-fold molar excess of the unlabeled oligonucleotide. This complex was supershifted in the presence of anti-PPAR- $\gamma$  antibody. Finally, Rtz increased luciferase activity in chondrocytes transiently transfected with a PPRE-luciferase gene reporter, in a dose-dependent manner from 0.1 to 1  $\mu$ M. Maximum activity (4-fold induction) was observed at 1  $\mu$ M and stayed in plateau up to 10  $\mu$ M (Fig. 1C).

**Low Concentrations of Rtz ( $\leq 1 \mu$ M) Selectively Inhibit IL-1 $\beta$ -induced Proteoglycan Degradation, Gelatinolytic Activities, and MMP1 Production**—Chondrocytes were incubated for 18 h in sulfate-free medium in the presence of <sup>35</sup>S-radiolabeled sulfate with or without effectors. <sup>35</sup>S-Sulfate incorporation into cetylpyridinium chloride-precipitable PG was measured in the culture medium. Fig. 2A shows that in the presence of IL-1 $\beta$  alone total <sup>35</sup>S-sulfated PG were decreased by 35  $\pm$  10%, from

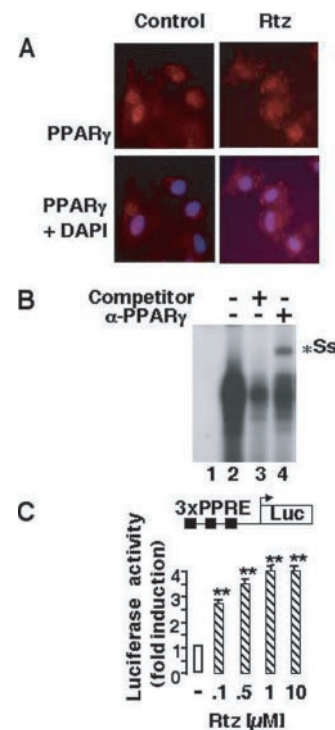


**FIG. 1. Cultured rabbit articular chondrocytes express a functional PPAR- $\gamma$ .** A, immunocytochemistry of PPAR- $\gamma$ . Rabbit articular chondrocytes were cultured at high density and incubated for 18 h in 2% FCS/DMEM in the absence (*Control*) or presence of 1  $\mu$ M Rtz (*Rtz*). Intracellular localization of PPAR- $\gamma$  was performed using an anti-PPAR- $\gamma$  antibody. PPAR- $\gamma$  localization appears predominantly nuclear independently of Rtz treatment of the cells. DAPI, 4,6-diamidino-2-phenylindole. B, EMSA. Nuclear extracts from chondrocytes incubated with 1  $\mu$ M Rtz were incubated with a [ $\gamma$ -<sup>32</sup>P]ATP-labeled oligonucleotide containing the canonical PPRE sequence from the acyl-CoA gene. Binding specificity was confirmed using an 80-fold molar excess of unlabeled oligonucleotide. A specific supershifted complex was observed in the presence of anti-PPAR- $\gamma$  antibody (\*Ss). C, transient expression. Chondrocytes were transiently transfected with a 3xPPRE-luciferase reporter plasmid and by  $\beta$ -galactosidase vector. Cells were treated with increasing concentrations of Rtz for 18 h (0.1–10  $\mu$ M). Cell extracts were assayed for luciferase activity. The activities were corrected for transfection efficiency by  $\beta$ -galactosidase activity and expressed as fold induction relative to the level in untreated cells. Each assay was performed in triplicate. Data are the mean  $\pm$  S.D. of three separate experiments performed with cells from different animals (\*\*,  $p \leq 0.01$  versus nontreated cells).

6.35  $\pm$  0.56 10<sup>4</sup> dpm/10  $\mu$ g DNA in control conditions to 4.12  $\pm$  0.39 10<sup>4</sup> dpm/10  $\mu$ g DNA ( $p < 0.01$ ). Addition of Rtz reproducibly induced a dose-dependent stimulation of <sup>35</sup>S-sulfated PG and fully restored control values at doses as low as 1  $\mu$ M, being stable at 10  $\mu$ M. These results show that low concentrations ( $\leq 1 \mu$ M) of Rtz counteract the detrimental effect of IL-1 $\beta$  on proteoglycans production.

We then asked whether this inhibitory effect involved the inhibition of the documented induction of matrix metalloproteinases production induced by IL-1 $\beta$  in chondrocytes. Among them MMP1 can be studied by gelatinolytic activity at an apparent molecular mass of 53/58 kDa. In our control conditions, chondrocytes secreted two main gelatinolytic activities at apparent molecular masses of 92 and 72 kDa, presumably corresponding to MMP9 and MMP2, respectively. Fig. 2B is representative of three separate experiments. Treatment with IL-1 $\beta$  alone caused an augmentation of the 92-kDa band and induced a new gelatinolytic activity at an apparent mass of 53–58 kDa, whereas no modification of the 72-kDa band was observed. Quantification analysis of the 92- and 53–58-kDa bands was done as relating to the 72-kDa band. The 92-kDa

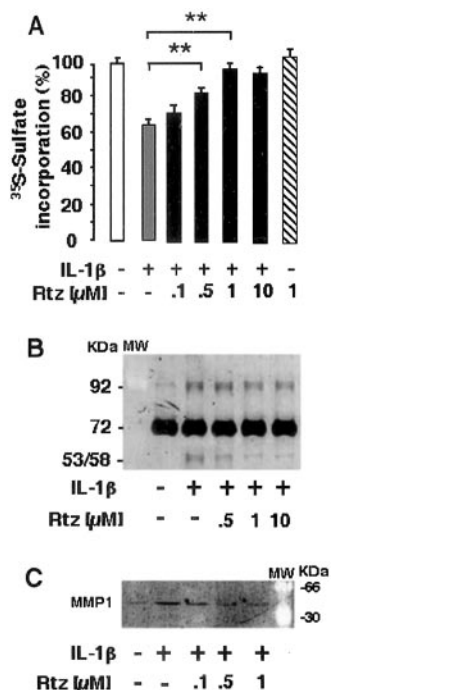


**FIG. 2. Low concentrations of Rtz selectively inhibit IL-1 $\beta$ -induced proteoglycan degradation, gelatinolytic activities, and MMP1 production.** Rabbit articular chondrocytes were cultured at high density and incubated for 18 h in 2% FCS/DMEM with or without 10 ng/ml IL-1 $\beta$  alone or combined with increasing concentrations of Rtz from 0.5 to 10  $\mu$ M. **A**, production of total <sup>35</sup>S-radiolabeled proteoglycans. Chondrocytes were cultured as described above. Total PG production was assayed after 18 h of incubation of the cells in sulfate-free medium containing either IL-1 $\beta$  alone or combined with increasing concentrations of Rtz. Each point was done in triplicate, and total PG was expressed as percent of nontreated cells. Data are mean  $\pm$  S.D. of five experiments performed with cells from different animal donors. \*\*,  $p < 0.01$  as compared with cells treated with IL-1 $\beta$  alone. **B**, gelatinolytic activities. Culture medium was collected and subjected to gelatin zymography as described under "Experimental Procedures." The levels of gelatinolytic bands were determined by scanning video densitometry. The 72-kDa band is not modified by IL-1 $\beta$  or Rtz and was used as internal control. **C**, Western blot confirmed the expression of MMP1 as a single band identified at  $\sim$ 55 kDa. This figure is representative of one of three separate experiments performed with different animals. Scanning densitometry of the MMP1 band observed in culture medium from chondrocytes treated with IL-1 $\beta$  alone or combined with 0.1, 0.5, or 1  $\mu$ M Rtz was compared with that observed in nontreated cells. Equal loading of protein was confirmed by Ponceau Red staining. Molecular mass marker sizes are indicated on the right.

gelatinolytic activity was decreased by  $40 \pm 3\%$  and by  $50 \pm 5\%$  ( $p < 0.01$ ) with 1 and 10  $\mu$ M Rtz, respectively. The IL-1 $\beta$ -induced 53/58-kDa gelatinolytic activity was decreased by  $35 \pm 5\%$  and by  $55 \pm 7\%$  ( $p < 0.01$ ) with 0.5 and 1 or 10  $\mu$ M Rtz, respectively. Similar results were observed at the protein level as shown by Western blot analysis. Fig. 2C is representative of three separate experiments. Scanning densitometry of the bands showed that the mean  $\pm$  S.D. of IL-1 $\beta$  overexpression of the MMP1 signal (apparent molecular mass, 52 kDa) was significantly decreased by Rtz in a dose-dependent manner, *i.e.* by  $41 \pm 3.8\%$  ( $p < 0.01$ ),  $70 \pm 11\%$  ( $p < 0.001$ ), and  $81 \pm 6\%$  ( $p < 0.001$ ), with 0.1, 0.5, or 1  $\mu$ M Rtz, respectively. These concurring data strongly suggest that the gelatinolytic activity observed at 53/58 kDa corresponds to the MMP1 protein.

**The Inhibitory Effect of Rtz on IL-1 $\beta$ -induced MMP1 mRNA Expression Is a Direct Mechanism**—Steady state levels of MMP1 mRNA were analyzed by Northern blotting, as compared with MMP3 and MMP13 mRNAs. As shown in Fig. 3A, MMP1, -3, and -13 mRNA levels were close to detection limits in control conditions, but were strongly expressed in the pres-

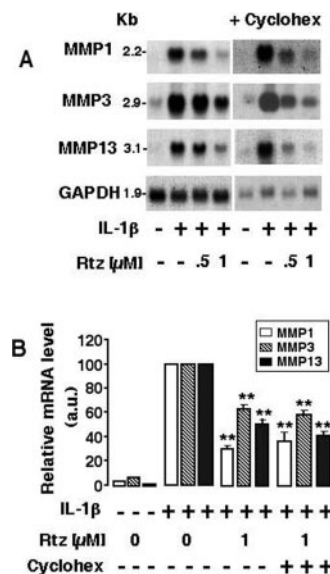


**FIG. 3. Low concentrations of Rtz counteract IL-1 $\beta$ -induced mRNA expression of MMP1, -3, and -13 by a direct mechanism.** Cells were incubated as described in Fig. 2, in the absence or presence of 1  $\mu$ M cycloheximide (*Cyclohex*). **A**, Northern blot. Total RNA (10  $\mu$ g) was subjected to Northern blotting and hybridized with rabbit MMPs probes. **B**, quantification of MMP1, -3, and -13 transcripts was performed by densitometric analysis of autoradiographs and normalized to the glyceraldehyde-3-phosphate dehydrogenase (*GAPDH*) signal. Data are means  $\pm$  S.D. of five separate experiments performed with chondrocytes from different animals (\*\*,  $p \leq 0.01$  versus IL-1 $\beta$ -treated cells).

ence of IL-1 $\beta$ . Co-treatment of Rtz and IL-1 $\beta$  decreased mRNA levels of MMP1, -3, and -13 by 25, 10, and 15%, respectively (0.5  $\mu$ M Rtz), and by 70, 40, and 55% (1  $\mu$ M Rtz) (Fig. 3B). This effect did not appear mediated by protein synthesis, as cycloheximide did not modify the inhibitory effect of Rtz on MMP1, -3, or -13 mRNA levels (Fig. 3A). These data suggest that down-regulation of IL-1 $\beta$ -induced proteoglycan degradation by Rtz may be mediated by inhibition of MMP production by chondrocytes. We then focused on the Rtz effect on *MMP1* gene transcription.

**The Inhibitory Effect of Rtz on IL-1 $\beta$ -induced MMP1 Gene Is Transcriptional and Requires PPAR- $\gamma$** —Chondrocytes were transiently transfected with a pMMP1-luciferase construct containing 3448 bp of the 5'-flanking region of the rabbit *MMP1* gene linked to the luciferase gene and supplemented with IL-1 $\beta$  and/or Rtz as described under "Experimental Procedures." Each point was done in triplicate, and this experiment was performed three times with different animals for the dose-response curve and twice for the dominant negative experiments. Fig. 4 showed that luciferase activity was not modified by addition of 1  $\mu$ M Rtz alone, whereas it was increased 4-fold by IL-1 $\beta$ . Co-treatment of chondrocytes with IL-1 $\beta$  and increasing concentrations of Rtz led to a dose-dependent reduction of *MMP1* promoter activity corresponding to  $23 \pm 3\%$  and  $42 \pm 3\%$  ( $n-1 = 17$ ,  $p < 0.001$ ) inhibition with 0.5 and 1  $\mu$ M Rtz, respectively, as compared with IL-1 $\beta$ -treated cells. In addition, a more pronounced inhibitory effect of Rtz ( $60 \pm 1\%$  inhibition,  $n-1 = 11$ ,  $p < 0.001$ ) was observed in cells overexpressing the wild type PPAR- $\gamma$ . The involvement of PPAR- $\gamma$  in the inhibitory effects of Rtz on *MMP1* transcription was further demonstrated by using a mutant dominant negative of PPAR- $\gamma$  (DN-PPAR- $\gamma$ ). Preliminary experiments showed that the DN-PPAR- $\gamma$  mutant abolishes the stimulatory effect of Rtz on a canonical PPRE-luciferase construct when co-expressed in chondrocytes (data not shown). As shown on Fig. 4, the inhibitory effect of Rtz on pMMP1-Luc activity was completely abolished by co-expression of DN-PPAR- $\gamma$ , supporting the implication of PPAR- $\gamma$  in this effect.

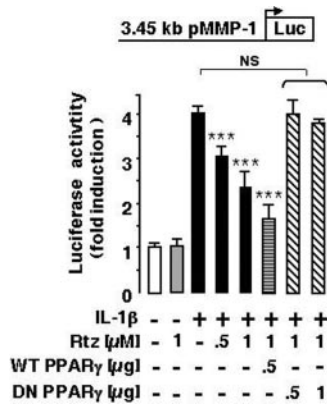


**FIG. 4. The inhibitory effect of Rtz on IL-1 $\beta$ -induced MMP1 gene involves PPAR- $\gamma$  at the transcriptional level.** Chondrocytes were transiently transfected with either the 3.45-kb pMMP1-luciferase (*Luc*) construct alone or combined with wild type (WT) PPAR- $\gamma$  or mutated dominant negative (DN) PPAR- $\gamma$  constructs and by  $\beta$ -galactosidase vector. Cells were treated with or without 1  $\mu$ M Rtz, 10 ng/ml IL-1 $\beta$ , or IL-1 $\beta$  combined with 0.5 or 1  $\mu$ M of Rtz for 18 h. Cell extracts were assayed for luciferase activity as in Fig. 1. The activities were corrected for transfection efficiency by  $\beta$ -galactosidase activity and expressed as fold induction relative to the level in untreated cells. Each point was done in triplicate, and this experiment was performed three times with different animals for the dose-response curve and twice for the dominant negative experiments. NS, not significant. Data are the means  $\pm$  S.D.; \*\*\*,  $p < 0.001$  versus IL-1 $\beta$ -treated cells.

*The Inhibitory Effect of Rtz on MMP1 Promoter Transcription Involves a Functional PPRE Situated at -83 to -71*—We have identified a degenerated PPRE sequence (AAAGCATGAGTCA) in the 3.45-bp region of the rabbit MMP1 promoter, located at -83 to -71 (GenBank<sup>TM</sup> accession number M17820). EMSA analysis showed the formation of a thin retarded complex between the PPRE and nuclear extract from nontreated chondrocytes (Fig. 5A, lane 1). Addition of Rtz strongly enhances this complex (Fig. 5A, lane 2). The specificity of binding activity was confirmed by competition experiments in the presence of an excess of either nonradioactive wild type PPRE or consensus PPRE oligonucleotide (ACOA sequence) (Fig. 5A, lanes 3 and 4). The signal was reduced and supershifted in the presence of an anti-PPAR- $\gamma$  antibody supporting the presence of PPAR- $\gamma$  in the complex (Fig. 5A, lane 5). Mutation into the PPRE sequence resulted in oligonucleotides displaying no PPAR- $\gamma$  binding activity and, consequently, no supershifted signal (Fig. 5A, lanes 6–9). Finally, the pMMP1-luciferase construct, bearing the mutated PPRE, was transiently transfected in chondrocytes. This experiment was done twice. Data shown on Fig. 5B showed that this mutation leads to the loss of Rtz inhibitory effect on IL-1 $\beta$ -mediated MMP1 transactivation. Together, these data demonstrate the following: (i) Rtz-activated PPAR- $\gamma$  binds the PPRE sequence situated at -83 to -71 in the MMP1 promoter, and (ii) PPAR- $\gamma$  binding is fundamental in the inhibition of IL-1 $\beta$ -induced MMP1 transcription by Rtz.

*The PPRE Sequence Situated at -83 to -71 in the MMP1 Promoter Is a Composite PPRE/AP1 Element and Promotes a Mutually Exclusive PPAR- $\gamma$  or AP1 Binding*—This -83/-71 PPRE sequence in the MMP1 promoter overlaps the proximal AP1 site at -77 (TGAGTCA), which is considered a key element in IL-1 $\beta$ -induced MMP1 expression. EMSA analysis using the composite PPRE/AP1 sequence was performed to highlight the respective involvement of AP1 and PPAR- $\gamma$  binding activity. As shown in Fig. 6A, nuclear extracts from chondrocytes treated with IL-1 $\beta$  alone elicited a DNA binding complex (lane 2) that was partly supershifted with either the anti-Fos family members (lane 3) or the specific anti-c-Jun

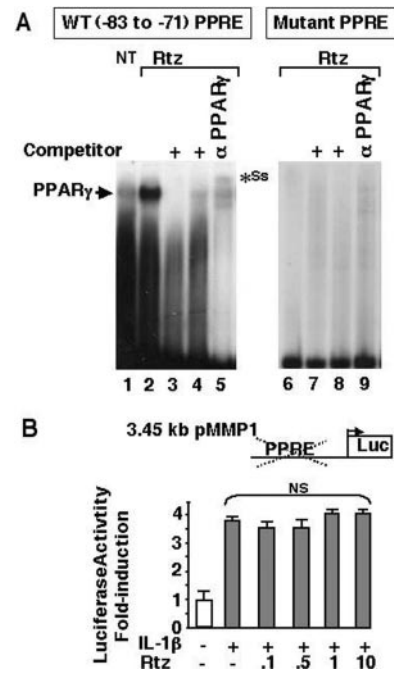


**FIG. 5. The functional PPRES sequence situated at -83 to -71 on the MMP1 promoter is required for PPAR- $\gamma$  binding and Rtz inhibitory effect.** A, EMSA. Nuclear extracts from nontreated (NT) chondrocytes (lane 1) or with 1  $\mu$ M Rtz (lanes 2–9) were prepared as described under “Experimental Procedures” and incubated with [ $\gamma$ -<sup>32</sup>P]ATP-labeled oligonucleotides containing the wild type (WT) -83 to -71 PPRES (lanes 1–5) or a mutated version of the PPRES sequence (lanes 6–9). Competition experiments were performed with a 100-fold molar excess of nonradioactive WT PPRES (lane 3), canonical PPRES sequence (lane 4), or a mutated PPRES (lanes 7 and 8). Identification of the complexes was done with an anti-PPAR- $\gamma$  antibody (lanes 5 and 9). \*Ss indicated the PPAR- $\gamma$  supershifted complex. B, transient expression. The 3.45-kb pMMP1-luciferase construct with the truncated -83 to -71 PPRES sequence was transiently transfected in chondrocytes as described in Fig. 4. Each point was performed in triplicate. Cells received 10 ng/ml IL-1 $\beta$  alone or combined with Rtz at concentrations ranging between 0.1 and 10  $\mu$ M. Luciferase assay was performed as in Fig. 4. Data are the means  $\pm$  S.D. of two separate experiments performed with cells from different animals. NS, not significantly different from IL-1 $\beta$ -treated cells.

antibody (lane 4). In order to characterize the nature of the Fos family member involved, we used specific antibodies against c-Fos, Fra-1, and Fra-2. The association of c-Fos and c-Jun antibodies totally supershifted the signal (Fig. 6A, lane 5). The isolated specific anti-c-Fos antibody substantially supershifted the signal (Fig. 6A, lane 6), whereas anti-Fra-1 or anti-Fra-2 were ineffective (lanes 7 and 8). In addition, the AP1 DNA binding complex was not supershifted upon addition of PPAR- $\gamma$  antibody (Fig. 6A, lane 9). These data show that IL-1 $\beta$ -induced AP1 complex contains c-Fos/c-Jun proteins but no PPAR- $\gamma$ -binding protein.

Another set of experiments was performed to study the fate of the AP1 complex when Rtz was added together with IL-1 $\beta$ . As seen on Fig. 6B, the AP1 complex observed with IL-1 $\beta$  alone (lane 1) was efficiently competed with a 50- and 100-fold molar excess of unlabeled -83/-71 PPRES sequence (lanes 2 and 3). By comparison, this complex was not elicited by nuclear extracts from chondrocytes co-treated with IL-1 $\beta$  and Rtz, whereas a new retarded species was observed (Fig. 6B, lane 4). This new band was competed with unlabeled -83/-71 PPRES sequence (Fig. 6B, lane 5) and was supershifted after addition of PPAR- $\gamma$  antibody (lane 6). No supershift of this complex was observed with PPAR- $\alpha$  (Fig. 6C, lane 3) nor PPAR- $\beta$  (lane 4) antibodies, indicating that PPAR- $\gamma$  was present in this new complex without other PPAR isotypes. Finally, neither c-Fos

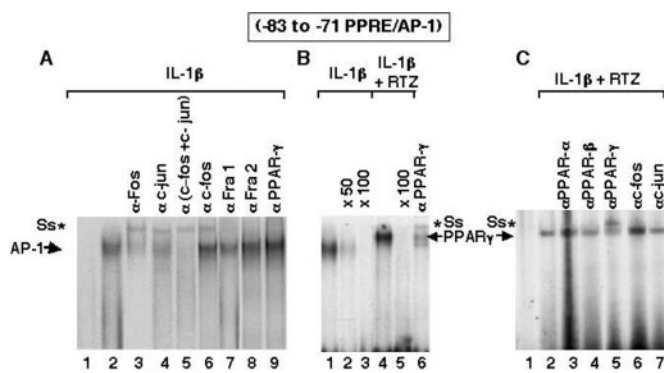


FIG. 6. PPAR $\gamma$  and AP1 binding to the PPRE sequence  $-83$  to  $-71$  of the *MMP1* promoter is mutually exclusive. EMSA. Nuclear extracts from chondrocytes either treated with IL-1 $\beta$  alone (A, lanes 2–9, and B, lanes 1–3) or with IL-1 $\beta$  plus Rtz (B, lanes 4–6, and C, lanes 2–7) were prepared and incubated with a [ $\gamma$ - $^{32}$ P]ATP-labeled oligonucleotide containing the  $-83$  to  $-71$  composite PPRE/AP-1 element of the rabbit *MMP1* promoter. Specificity of binding was confirmed using 50- (B lane 2) or 100-fold (B, lanes 3 and 5) molar excess of unlabeled corresponding oligonucleotide. Identification of each complex was done with the following antibodies: anti-Fos family members (A, lane 3), anti-c-Jun (A, lane 4, and C, lane 7), anti-c-Fos plus anti-c-Jun (A, lane 5), anti-c-Fos (A, lane 6, and C, lane 6), anti-Fra-1 (A, lane 7), anti-Fra-2 (A, lane 8), and anti-PPAR- $\gamma$  (A, lane 9, and B, lane 6, and C, lane 5), anti-PPAR- $\alpha$  (C, lane 3), and anti-PPAR- $\beta$  (C, lane 4) antibodies. A and C, lanes 1 are with radiolabeled  $-83$  to  $-71$  PPRE element alone. \*Ss indicated the supershifted signal of each corresponding DNA complex.

nor c-Jun antibodies (Fig. 6C, lanes 6 and 7) modified this signal, confirming the absence of AP1 proteins in this complex. Taken together, these data demonstrate a mutually exclusive binding of PPAR- $\gamma$  and AP1 to the composite element  $-83$  to  $-71$  of *MMP1* promoter.

We then investigated whether the PPAR $\gamma$  inhibitory effect on IL-1 $\beta$ -induced *MMP1* transcription might involve NF- $\kappa$ B transcription factors. EMSA analysis (Fig. 7) using an oligonucleotide bearing the  $-3029$  NF $\kappa$ B-RE motif from the *MMP1* promoter showed that no complex was observed using nuclear extracts from nontreated or Rtz-treated cells (lanes 1 and 2). IL-1 $\beta$  treatment of chondrocytes elicited the formation of two DNA binding complexes (Fig. 7, lane 3), which were mostly supershifted with anti-P50 antibodies (lane 4). The lower mobility band was partly supershifted with anti-P65, whereas the higher mobility band was not modified (Fig. 7, lane 5). These data indicate that the lower mobility band mainly consists of the p65-p50 heterodimer, whereas a p50 homodimer is present in the higher mobility band. Rtz treatment had no significant effect on any complex (lanes 6–8). In conclusion, no detectable cross-talk occurs between IL-1 $\beta$ -induced NF- $\kappa$ B binding activity and Rtz-activated PPAR- $\gamma$  at the  $-3029$  NF $\kappa$ B-RE.

#### DISCUSSION

We report here on the anti-cytokine effects of PPAR- $\gamma$  activation in rabbit cartilage cells. Low concentrations ( $\leq 1$   $\mu$ M) of the classical pharmacological ligand Rtz selectively inhibit IL-1 $\beta$ -induced proteoglycan degradation and *MMP1* expression. The latter Rtz inhibitory effect targets the rabbit *MMP1* promoter via a novel composite element. PPAR- $\gamma$  is constitutively expressed in cultured rabbit articular chondrocytes as shown by immunocytochemistry in Fig. 1A. EMSA experiments and chondrocyte transient transfections with a 3X-PPRE-Luciferase construct demonstrated that endogenous PPAR- $\gamma$  is functionally activated by low doses of Rtz (0.1–1  $\mu$ M) with a maximum activity at 1  $\mu$ M (Fig. 1B). This is at variance with the results of Fahmi *et al.* (3) who found a maximum stimulating effect of such a reporter construct in cultured human chondrocytes by using a 100-fold higher concentration of Rtz. This discrepancy may relate to a lower PPAR- $\gamma$  content in cultured

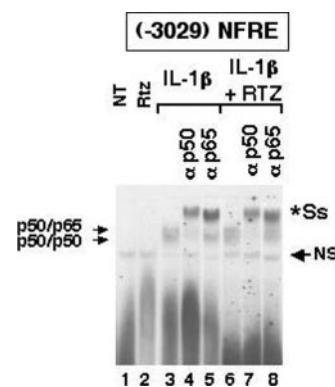


FIG. 7. No detectable cross-talk occurs between IL-1 $\beta$ -induced NF- $\kappa$ B binding activity and Rtz-activated PPAR- $\gamma$  at the  $-3029$  NF $\kappa$ B-RE of *MMP1* promoter. EMSA. Nuclear extracts from chondrocytes incubated in basal conditions (lane 1), treated with Rtz alone (lane 2), with IL-1 $\beta$  alone (lanes 3–5), or with IL-1 $\beta$  + Rtz (lanes 6–8) were prepared and incubated with [ $\gamma$ - $^{32}$ P]ATP-labeled oligonucleotide containing the  $-3029$  NF $\kappa$ B-RE. Identification of the NF- $\kappa$ B complexes was done with anti-p50 (lanes 4 and 7) and anti-p65 (lanes 5 and 8) antibodies. \*Ss indicated the supershifted signal of each corresponding DNA complex. NS indicated a nonspecific complex.

human chondrocytes compared with rabbit cells.

We studied the effects of Rtz on a series of IL-1 $\beta$ -induced genes. Low concentrations of Rtz (0.1 to 1  $\mu$ M) negatively regulated specific subsets of IL-1 $\beta$ -induced effects in chondrocytes, whereas Rtz alone displayed no effect. A significant decrease of proteoglycan degradation was associated with down-regulation of 53/58-kDa gelatinolytic activity, *MMP1* mRNA expression, and *MMP1* protein production (Fig. 2). Most interesting, low concentrations of Rtz did not affect IL-1 $\beta$ -induced COX $_2$  mRNA expression nor nitrite production, whereas both inflammatory markers, as well as *MMP1* expression, were reduced with high doses (10  $\mu$ M) of Rtz (data not shown). This pharmacological variance supports the notion that Rtz differently modulates IL-1 $\beta$ -induced inflammation and degradation in cartilage cells. Inhibition of MMPs by low concentrations of natural as well as synthetic PPAR- $\gamma$  ligands has also been reported in other models (14, 29–32). The PPAR- $\gamma$  mediation of MMPs inhibition has been described but not fully demonstrated. We have investigated the mechanism of the inhibitory effect of Rtz with a focus on IL-1 $\beta$ -induced *MMP1* in chondrocytes.

The repression of IL-1 $\beta$ -induced *MMP1* overexpression by Rtz is dose-dependent, direct, and occurs at the transcriptional level, as observed by transient expression experiments using the p*MMP1*-Luc vector (Fig. 4). In addition, the Rtz inhibitory effect was enhanced in chondrocytes transiently transfected with the wild type PPAR- $\gamma$ , whereas it was abolished in cells transfected with a dominant negative mutant PPAR- $\gamma$ . This further supports the implication of PPAR- $\gamma$  in the inhibitory effect of Rtz. PPAR- $\gamma$  has been shown to modulate IL-1 $\beta$ -induced genes by several mechanisms including protein-protein (NF- $\kappa$ B, AP1, STAT) or DNA-protein interactions. Chung *et al.* (33) have shown that PPAR- $\gamma$  inhibits NF- $\kappa$ B-driven transcription by physically interacting with p50 and p65 proteins as reported previously by Delerive *et al.* (34) for PPAR- $\alpha$ . An NF- $\kappa$ B-responsive element has been characterized at position  $-3029$  to  $-2994$  in the *MMP1* promoter, which is required for maximal IL-1 $\beta$  transcriptional induction in synovial fibroblasts (23). In the present study, the  $-3029$  to  $-2994$  NF $\kappa$ B-RE is shown to form DNA complexes involving p50/p50 homodimer and p50/p65 heterodimer proteins. The binding activity of these complexes was not modified in the presence of Rtz (Fig. 7), suggesting that Rtz-activated PPAR- $\gamma$  does not interfere with IL-1 $\beta$ -induced NF- $\kappa$ B binding activity in our model.

Activated PPAR- $\gamma$  also acts through DNA binding interaction with its cognate PPRE sequences (direct repeats with single spacing nucleotide, DR1) located in the promoter of target genes. For example, the activated PPAR- $\gamma$  inhibits regulated on activation normal T cell expressed and secreted (RANTES) transcription and protein production in endometriotic stromal cells through a specific PPRE at -334 to -322 upstream from the RNA polymerase start site (35). We have identified a degenerated DR1 sequence (AAAGCATGAGTCA) located at -83 to -71 in the rabbit *MMP1* promoter. Gel mobility shift and supershift assays showed that this *cis*-acting element binds PPAR- $\gamma$ , whereas no binding activity was observed with a mutated PPRE (Fig. 5A). In addition, Rtz failed to inhibit *MMP1* promoter activity when chondrocytes were transfected with a p*MMP1*-Luc vector bearing this mutated PPRE (Fig. 5B). Altogether these data demonstrate that the inhibitory effect of Rtz on IL-1 $\beta$ -induced *MMP1* gene transcription implicates PPAR- $\gamma$  binding on the -83 to -71 *cis*-acting sequence of the *MMP1* promoter.

The next question was to study whether the reduced IL-1 $\beta$ -induced *MMP1* expression by Rtz was because of an interaction between PPAR- $\gamma$  and AP1 binding activities on the -83 -71 sequence of the *MMP1* promoter. Fahmi *et al.* (36) have shown previously that 15d-PGJ2, a lower affinity PPAR- $\gamma$  ligand, reduces IL-1 $\beta$ -induced *MMP1* expression in human synovial fibroblasts and inhibits AP1 DNA binding activity. They concluded that 15d-PGJ2 negatively regulated *MMP1* expression by interfering with AP1 activation, although neither the PPAR- $\gamma$  dependence of the 15d-PGJ2 inhibitory effect nor the PPAR- $\gamma$ /AP1 interactions were analyzed. Their EMSA experiment describing the decreased AP1 binding activity was performed with an oligonucleotide corresponding to the restricted AP1 sequence -77-71 of the *MMP1* promoter, which does not comprise the full overlapping PPRE -83-71 sequence. In addition, BRL49653 (Rtz) was much less effective than 15d-PGJ2, with an inhibitory effect only observed at very high concentrations (10-100  $\mu$ M) far from its  $K_d$  value for PPAR- $\gamma$ , and no information was provided about the effect of Rtz on the AP1 binding activity. Altogether these data supported a PPAR- $\gamma$ -independent pathway for the anti-*MMP1* effect of the 15d-PGJ2. Indeed, 15d-PGJ2 has been shown to reduce AP1 activation in several anti-inflammatory responses by interacting at multiple levels along the AP1 pathway (37). More recently, Mix *et al.* (38) showed that 15d-PGJ2 decreased IL-1 $\beta$ -induced *MMP1* expression in the human SW-1353 chondrosarcoma cell line, through a novel PPAR- $\gamma$ -independent mechanism that requires Smad signaling.

In the present work, a series of EMSA analyses were performed with the composite PPRE/AP1 element in order to highlight the respective involvement of PPAR- $\gamma$  and AP1 binding activities, in cells co-treated with IL-1 $\beta$  and Rtz (Fig. 6). The IL-1 $\beta$ -induced AP1 DNA binding activity observed in chondrocytes was shown to contain immunoreactive c-Fos and c-Jun proteins (Fig. 6A). This is at variance with the AP1 complex induced in fibroblast growth factor-stimulated *MMP1* in MC3T3-E1 osteoblasts and in PMA-induced *MMP1* in rabbit fibroblasts (39, 40). In these cases, the AP1 complex was shown to contain Fra-1- or Fra-2-binding proteins at the -77 site of the *MMP1* promoter. However, our data are in accordance with those from Chamberlain *et al.* (41) and Hamid *et al.* (42) who showed an up-regulation of *MMP1* by PMA or IL-1 $\beta$  involving a c-Fos-c-Jun AP1 complex at -77 to -69 of the promoter. Finally, the IL-1 $\beta$ -induced complex bound to the AP1 element, characterized under the present experimental conditions, was not recognized by anti-PPAR- $\gamma$  antibodies indicating the absence of PPAR- $\gamma$  proteins in this complex.

When nuclear extracts were prepared from IL-1 $\beta$  and Rtz co-treated cells, the AP1 complex totally disappeared, whereas a differently shifted complex was observed (Fig. 6B). This new complex is further supershifted in the presence of an anti-PPAR- $\gamma$  antibody but not with c-Fos and c-Jun antibodies and not with PPAR- $\alpha$  or PPAR- $\beta$  antibodies, indicating that this complex only contain PPAR- $\gamma$  (Fig. 6C). Taken together, our data demonstrate that AP1 and PPAR- $\gamma$  bindings on the composite PPRE/AP1 sequence are mutually exclusive.

Our data are consistent with a new PPAR- $\gamma$ -dependent inhibitory mechanism of Rtz on IL-1 $\beta$ -induced *MMP1* expression in chondrocytes. This inhibition appears to be mediated through binding competition between PPAR- $\gamma$  and the AP1 complex for the composite PPRE/AP1 at position -83 to -71. As direct repeat (DR1) *cis*-acting elements can be recognized by a variety of transcription factors including the chicken ovalbumin upstream promoter-transcription factor or RAR-related orphan receptor (43), we cannot exclude the possibility that in our model other transcription factors may also bind this composite element and take part into the transcriptional down-regulation of the *MMP1* gene.

Whether PPAR- $\gamma$ -dependent inhibition is restricted to *MMP1* or occurs with other MMPs remains to be investigated. In the present work Rtz was shown to inhibit IL-1 $\beta$ -induced MMP9 gelatinolytic activities and MMP3 and MMP13 mRNA levels. PPAR- $\gamma$  agonists were also found to inhibit *MMP3* expression in human rheumatoid fibroblast-like synoviocytes (44). Down-regulation of MMP9 by natural (15d-PGJ2) and synthetic (GW7845) PPAR- $\gamma$  ligands in PMA-stimulated THP-1 monocytes has been consistently observed (31). An inhibition of *MMP13* expression by Rtz was also reported by Fahmi *et al.* (3) in human chondrocytes. Similarly to the *MMP1* gene situation, AP1 has been shown to be involved in the up-regulation of *MMP3* in meshwork cells (45), *MMP9* in human vascular smooth muscle cells (46), and *MMP13* in osteoblasts (27). We searched for the presence of a DR1-PPRE overlapping an AP1 element in the promoter of *MMP3*, *MMP9*, and *MMP13*. An AP-1 site at position -1929 and a PPRE at position -1950 have been recently identified in the murine *MMP3* (47). Computer analysis of the human *MMP3* (GenBank<sup>TM</sup> accession number AF405705) allowed us to identify a degenerated DR1-PPRE overlapping an AP1 element at position -73 to -63 (CAAGGATGAGTCA). Two PPRES were recently identified in the rat *MMP9* promoter (48). Most interesting, we found a degenerated PPRES overlapping an AP1 element (TGAGTCAGAAGTTTCG) at position -1661 to -1646 in the human *MMP9* promoter (GenBank<sup>TM</sup> accession number AF538844). Finally, we found a DR1-PPRE/AP1 sequence (AAGT-GATGACTCA) at position -80 to -67 in the human (GenBank<sup>TM</sup> accession number X81640), rat (GenBank<sup>TM</sup> accession number AY135636), and dog (GenBank<sup>TM</sup> accession number AF384859) promoters of *MMP13*. We thus speculated that the Rtz inhibitory effect on IL-1 $\beta$ -induced *MMP3*, -9, and -13 may occur through a mechanism similar to the Rtz effect on *MMP1*.

In conclusion, we have determined that Rtz-activated PPAR- $\gamma$  represses *MMP1* transcription in chondrocytes, by interfering with the binding of c-Fos/c-Jun proteins to the promoter sequences situated at -83-71. Further studies will be performed to confirm that this interaction occurs *in vivo* in the chromatin environment and to determine whether other co-factors participate in this effect. Nevertheless, PPAR- $\gamma$  appears able to counteract the IL-1 $\beta$ -induced proteoglycan degradation and *MMP1* transcription acting as a protective mechanism in cartilage. This beneficial function can be elicited by low concentrations of Rtz (and probably other thiazolidinediones), in contrast with the much less manageable

amounts required with most other PPAR- $\gamma$  ligands. Thiazolidinediones thus deserve consideration for clinical testing in degenerative cartilage diseases.

**Acknowledgments**—We thank Dr. Steve Smith (GlaxoSmithKline, UK) for providing us with BRL 49653 (Rtz) and Dr. Paul Grimaldi (Nice, France) for the PPRESX3-TK-Luc construct.

## REFERENCES

- Kawahito, Y., Kondo, M., Tsubouchi, Y., Hashiramoto, A., Bishop-Bailey, D., Inoue, K., Kohno, M., Yamada, R., Hla, T., and Sano, H. (2000) *J. Clin. Invest.* **106**, 189–197
- Boyvaut, S., Simonin, M. A., Bianchi, A., Compe, E., Liagre, B., Mainard, D., Becuwe, P., Dauca, M., Netter, P., Terlain, B., and Bordji, K. (2001) *FEBS Lett.* **501**, 24–30
- Fahmi, H., Di Battista, J. A., Pelletier, J. P., Mineau, F., Ranger, P., and Martel-Pelletier, J. (2001) *Arthritis Rheum.* **44**, 595–607
- Sabatini, M., Bardiot, A., Lesur, C., Moulharat, N., Thomas, M., Richard, I., and Fradin, A. (2002) *Osteoarthritis Cartilage* **10**, 673–679
- Henderson, B., and Pettipher, E. R. (1989) *Clin. Exp. Immunol.* **75**, 306–310
- Cooper, W. O., Fava, R. A., Gates, C. A., Cremer, M. A., and Townes, A. S. (1992) *Clin. Exp. Immunol.* **89**, 244–250
- Issemann, I., and Green, S. (1990) *Nature* **347**, 645–650
- Willson, T. M., Lambert, M. H., and Kliewer, S. A. (2001) *Annu. Rev. Biochem.* **70**, 341–367
- Lapillonne, H., Konopleva, M., Tsao, T., Gold, D., McQueen, T., Sutherland, R. L., Madden, T., and Andreoff, M. (2003) *Cancer Res.* **63**, 5926–5939
- Jiang, C., Ting, A. T., and Seed, B. (1998) *Nature* **391**, 82–86
- Marx, N., Sukhova, G., Murphy, C., Libby, P., and Plutzky, J. (1998) *Am. J. Pathol.* **153**, 17–23
- Ricote, M., Li, A. C., Willson, T. M., Kelly, C. J., and Glass, C. K. (1998) *Nature* **391**, 79–82
- Su, C. G., Wen, X., Bailey, S. T., Jiang, W., Rangwala, S. M., Keilbaugh, S. A., Flanigan, A., Murthy, S., Lazar, M. A., and Wu, G. D. (1999) *J. Clin. Invest.* **104**, 383–389
- Marx, N., Mach, F., Sauty, A., Leung, J. H., Sarafi, M. N., Ransohoff, R. M., Libby, P., Plutzky, J., and Luster, A. D. (2000) *J. Immunol.* **164**, 6503–6508
- Huang, J. T., Welch, J. S., Ricote, M., Binder, C. J., Willson, T. M., Kelly, C., Witztum, J. L., Funk, C. D., Conrad, D., and Glass, C. K. (1999) *Nature* **400**, 378–382
- Daynes, R. A., and Jones, D. C. (2002) *Nat. Rev. Immunol.* **2**, 748–759
- Chawla, A., Barak, Y., Nagy, L., Liao, D., Tontonoz, P., and Evans, R. M. (2001) *Nat. Med.* **7**, 48–52
- Straus, D. S., Pascual, G., Li, M., Welch, J. S., Ricote, M., Hsiang, C. H., Sengchanthalangsy, L. L., Ghosh, G., and Glass, C. K. (2000) *Proc. Natl. Acad. Sci. U. S. A.* **97**, 4844–4849
- Rossi, A., Kapahi, P., Natoli, G., Takahashi, T., Chen, Y., Karin, M., and Santoro, M. G. (2000) *Nature* **403**, 103–108
- Castrillo, A., Diaz-Guerra, M. J., Hortelano, S., Martin-Sanz, P., and Bosca, L. (2000) *Mol. Cell. Biol.* **20**, 1692–1698
- Corvol, M. T., Dumontier, M. F., and Rappaport, R. (1975) *Biomedicine (Paris)* **23**, 103–107
- Riquet, F. B., Tan, L., Choy, B. K., Osaki, M., Karsenty, G., Osborne, T. F., Auron, P. E., and Goldring, M. B. (2001) *J. Biol. Chem.* **276**, 38665–38672
- Vincenti, M. P., Coon, C. I., and Brinckerhoff, C. E. (1998) *Arthritis Rheum.* **41**, 1987–1994
- Corvol, M. T., Carrascosa, A., Tsagris, L., Blanchard, O., and Rappaport, R. (1987) *Endocrinology* **120**, 1422–1429
- Larsson, S. E., and Kuettner, K. E. (1974) *Calcif. Tissue Res.* **14**, 49–58
- Kapuscinski, J., and Skoczylas, B. (1977) *Anal. Biochem.* **83**, 252–257
- Hess, J., Porte, D., Munz, C., and Angel, P. (2001) *J. Biol. Chem.* **276**, 20029–20038
- Gurnell, M., Wentworth, J. M., Agostini, M., Adams, M., Collingwood, T. N., Provenzano, C., Browne, P. O., Rajanayagam, O., Burris, T. P., Schwabe, J. W., Lazar, M. A., and Chatterjee, V. K. (2000) *J. Biol. Chem.* **275**, 5754–5759
- Haffner, S. M., Greenberg, A. S., Weston, W. M., Chen, H., Williams, K., and Freed, M. I. (2002) *Circulation* **106**, 679–684
- Shu, H., Wong, B., Zhou, G., Li, Y., Berger, J., Woods, J. W., Wright, S. D., and Cai, T. Q. (2000) *Biochem. Biophys. Res. Commun.* **267**, 345–349
- Worley, J. R., Baugh, M. D., Hughes, D. A., Edwards, D. R., Hogan, A., Sampson, M. J., and Gavrilovic, J. (2003) *J. Biol. Chem.* **278**, 51340–51346
- Hetzel, M., Walcher, D., Grub, M., Bach, H., Hombach, V., and Marx, N. (2003) *Thorax* **58**, 778–783
- Chung, S. W., Kang, B. Y., Kim, S. H., Pak, Y. K., Cho, D., Trinchieri, G., and Kim, T. S. (2000) *J. Biol. Chem.* **275**, 32681–32687
- Delerive, P., De Bosscher, K., Besnard, S., Vanden Berghe, W., Peters, J. M., Gonzalez, F. J., Fruchart, J. C., Tedgui, A., Haegeman, G., and Staels, B. (1999) *J. Biol. Chem.* **274**, 32048–32054
- Pritts, E. A., Zhao, D., Sohn, S. H., Chao, V. A., Waite, L. L., and Taylor, R. N. (2003) *Fertil. Steril.* **80**, 415–420
- Fahmi, H., Pelletier, J. P., Di Battista, J. A., Cheung, H. S., Fernandes, J. C., and Martel-Pelletier, J. (2002) *Osteoarthritis Cartilage* **10**, 100–108
- Perez-Sala, D., Cernuda-Morollon, E., and Canada, F. J. (2003) *J. Biol. Chem.* **278**, 51251–51260
- Mix, K. S., Coon, C. I., Rosen, E. D., Suh, N., Sporn, M. B., and Brinckerhoff, C. E. (2004) *Mol. Pharmacol.* **65**, 309–318
- Newberry, E. P., Willis, D., Latifi, T., Boudreaux, J. M., and Towler, D. A. (1997) *Mol. Endocrinol.* **11**, 1129–1144
- White, L. A., and Brinckerhoff, C. E. (1995) *Matrix Biol.* **14**, 715–725
- Chamberlain, S. H., Hemmer, R. M., and Brinckerhoff, C. E. (1993) *J. Cell. Biochem.* **52**, 337–351
- Hamid, Q. A., Reddy, P. J., Tewari, M., Uematsu, S., Tuncay, O. C., and Tewari, D. S. (2000) *Cytokine* **12**, 1609–1619
- Tsai, S. Y., and Tsai, M. J. (1997) *Endocr. Rev.* **18**, 229–240
- Yamasaki, S., Nakashima, T., Kawakami, A., Miyashita, T., Ida, H., Migita, K., Nakata, K., and Eguchi, K. (2002) *Clin. Exp. Immunol.* **129**, 379–384
- Fleener, D. L., Pang, I. H., and Clark, A. F. (2003) *Investig. Ophthalmol. Vis. Sci.* **44**, 3494–3501
- Moon, S. K., Cha, B. Y., and Kim, C. H. (2004) *J. Cell. Physiol.* **198**, 417–427
- Yee, J., Kuncio, G. S., Bhandari, B., Shihab, F. S., and Neilson, E. G. (1997) *Kidney Int.* **52**, 120–129
- Eberhardt, W., Akool el, S., Rebhan, J., Frank, S., Beck, K. F., Franzen, R., Hamada, F. M., and Pfeilschifter, J. (2002) *J. Biol. Chem.* **277**, 33518–33528



**Peroxisome Proliferator-activated Receptor- $\gamma$  Down-regulates Chondrocyte Matrix Metalloproteinase-1 via a Novel Composite Element**

Mathias François, Pascal Richette, Lydia Tsagris, Michel Raymondjean, Marie-Claude Fulchignoni-Lataud, Claude Forest, Jean-François Savouret and Marie-Thérèse Corvol

*J. Biol. Chem.* 2004, 279:28411-28418.

doi: 10.1074/jbc.M312708200 originally published online April 16, 2004

---

Access the most updated version of this article at doi: [10.1074/jbc.M312708200](https://doi.org/10.1074/jbc.M312708200)

Alerts:

- [When this article is cited](#)
- [When a correction for this article is posted](#)

[Click here](#) to choose from all of JBC's e-mail alerts

This article cites 48 references, 16 of which can be accessed free at <http://www.jbc.org/content/279/27/28411.full.html#ref-list-1>